

Electronic Supplementary Material (ESI[†])

Effect of Two-fold Single-atom Substitutions (S, Se; C, N) in Band Gap Engineered Donor-Acceptor Conjugated Microporous Polymers on Efficient Aerobic Photooxidation of Aryl Sulfides

Soumitra Sau, Suman Karmakar,[#] Flora Banerjee[#] and Suman Kalyan Samanta*

Department of Chemistry, Indian Institute of Technology Kharagpur, Kharagpur 721302, India. E-mail: sksamanta@chem.iitkgp.ac.in

1. Experimental Section

1.1. Materials and Methods. All the chemicals and reagents were purchased from commercial sources and used directly as raw materials without further treatment. Thin layer chromatography (TLC) on silica gel GF254 was used for the determination of R_f values and the visualization was performed by irradiation with UV lamp at 254 nm. Column chromatography was performed on Merck silica gel (100-200 mesh) with eluent as mentioned. ^1H (500 MHz) and ^{13}C (125 MHz) NMR spectra were recorded in a Bruker advance-500 NMR spectrometer in deuterated solvent at ambient temperature (300 K). Chemical shifts are reported in ppm (δ) relative to tetramethylsilane (TMS) as the internal standard (CDCl_3 δ 7.26 ppm for ^1H and 77.0 ppm for ^{13}C). Solid state ^{13}C CPMAS NMR spectra were recorded in a Bruker Ultrashield-500 NMR spectrometer. Fourier transform infrared spectra (FTIR, 4000-600 cm^{-1}) were performed on Nicolet 6700 FT-IR spectrometer (Thermo Fischer) instrument, the wave numbers of recorded IR signals are reported in cm^{-1} . Thermogravimetric analyses (TGA) were performed on a Pyris Diamond TG DTA (PerkinElmer) instrument. The as-synthesized D-A CMPs were observed under scanning electron microscope (SEM) model ZEISS SUPRA 40. The samples were prepared on gold stubs by adding powder polymers mounted on top of double-sided tapes. UV-Vis-NIR diffuse reflection spectrum (DRS) was acquired with UV-Vis-NIR spectrophotometer (Cary 5000, Agilent). X-Ray diffraction patterns of the powder organic polymer samples were obtained using a Bruker AXS D-8Advanced SWAX diffractometer using $\text{Cu-K}\alpha$ (0.15406 nm) radiation. Solid-state PL emission studies were recorded on a fluorescence spectrophotometer (Jobin Yvon-Spex Fluorolog-3). The time-resolved fluorescence lifetime was measured with a time-correlated single photon counting (TCSPC) device. A picoseconds diode laser (IBH, UK, Nanoled) was used as a light source at the excitation wavelength of 440 nm. The signal was detected in magic angle (54.7°) polarization using a Hamamatsu MCP PMT (3809U) and the decays were analyzed using IBH DAS-6 decay analysis software. The N_2 adsorption/desorption isotherms of the sample were recorded on a Micromeritics 3-Flex Surface Characterization Analyzer at 77 K. UV-visible absorption spectra were recorded on a Shimadzu UV-2550 UV-Vis spectrophotometer. The specific measurement details regarding reactive oxygen species (ROS) trapping are as follows: In 3 mL air-saturated CH_3CN , 5 mg photocatalyst and 5 mg of N,N,N',N' -tetramethylphenylenediamine (NTPD) were added. Then O_2 was purged into that mixture and stirred the whole mixture under white light irradiation (100 W white LED) for 2 h. Then, the polymer was filtered out and the filtrate portion was submitted for UV. Bruker ELEXSYS 580 spectrometer was used to record the EPR spectra. The specific measurement details regarding reactive oxygen species (ROS) trapping are as follows: the modulation frequency = 100.00 kHz, modulation amplitude = 5.000 G. The samples were prepared by adding 1 mg of photocatalyst to a 1 mL 0.1 M air-saturated methanol solution of 5,5-dimethyl-1-pyrrolineN-oxide (DMPO).

1.2. Electrochemical measurements

Cyclic voltammetry (CV) measurement was carried out by using a CH instrument with three electrode-cell [CMPs-coated glassy carbon electrode as a working electrode, platinum wire as a counter electrode, and Ag/Ag⁺ in acetonitrile (+0.49 V vs NHE)¹ as a reference electrode. A scan rate of 0.1 V/s was used. A solution of 0.1 (M) tetrabutylammonium hexafluorophosphate in acetonitrile was used as the supporting electrolyte. 2 mg of well-dried POPs was well dispersed in a binder solution of 25 wt% of polyvinylidene fluoride (PVDF) and 500 μ L of ethanol through ultrasonication for 1 h to obtain a stable suspension. Then the pre-polished glassy carbon electrode was coated by 20 μ L of the prepared polymeric dispersion. The electrode was dried for one day at room temperature and then prior to CV experiment. The electrode potential values are given with respect to $E_{\text{Ag/AgCl}} = 0.197$ vs NHE.² The LUMO energy levels of the POPs were determined by using the empirical equations, $E_{\text{LUMO}} = (E_{\text{onset/red}} + 0.49 - 0.197)$ V (vs Ag/AgCl).^{3,4} EIS was determined over the frequency range of 10^2 – 10^6 Hz with an ac amplitude of 10 mV at the open circuit voltage under room-light illumination by using 0.5 M Na₂SO₄ aqueous solution as supporting electrolyte.

1.3. Photocurrent measurements

Photoelectrochemical measurements were conducted in a three-electrode system using CH instrument under 20 W white LED. The working electrodes are prepared as follows: 2 mg of well dried CMPs is separately ground with 0.5 mg of polyvinylidene fluoride (PVDF) and 50 μ L of ethanol to make slurry. The slurry is then coated onto FTO glass electrodes with an active area of 1 cm², and these electrolytes were dried at 80 °C for 1 h to evaporate the solvent. An aqueous solution of 0.5 M Na₂SO₄ was used as the supporting electrolyte. The photocurrent intensity of the as-prepared electrodes was measured at 0.3 V versus s-Ag/AgCl with the light on and off.

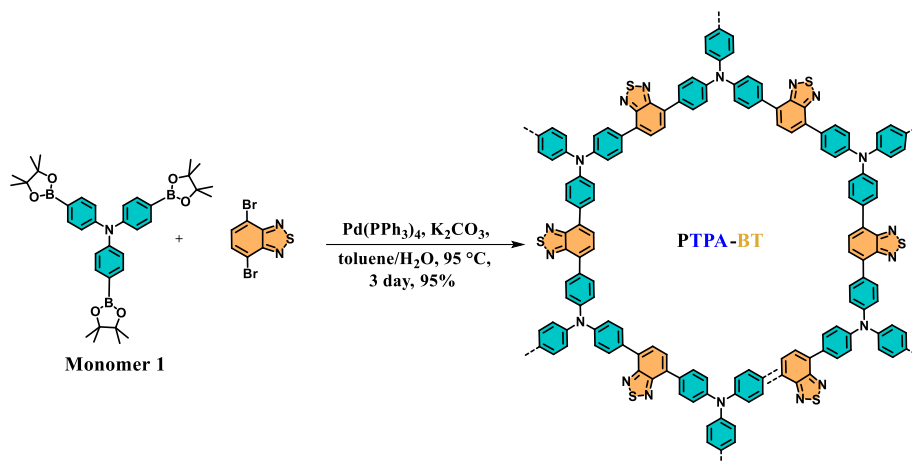
Synthetic Procedure

Synthesis of D-A CMPs:

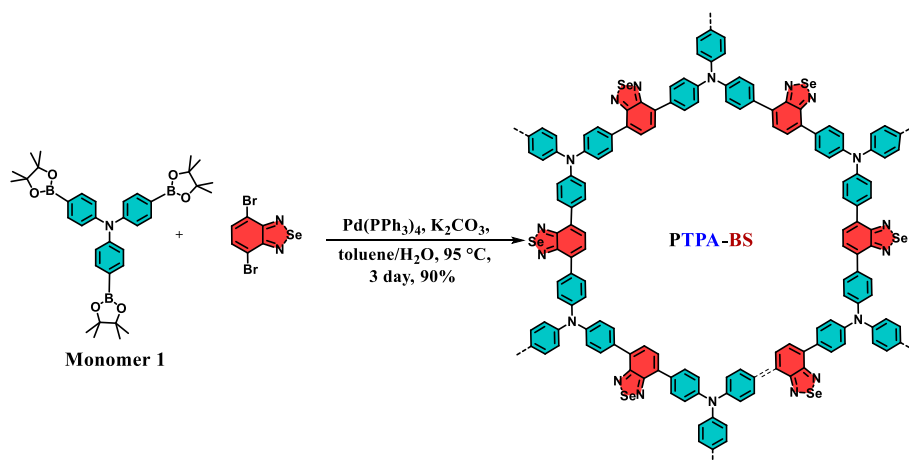
Synthesis of PTPA-BT:

PTPA-BT was synthesized following a previously reported procedure with slight modification. In a 50 mL two-necked round-bottom flask, monomer **1** (250 mg, 0.401 mmol), 4,7-dibromo-2,1,3-benzothiadiazole (176 mg, 0.602 mmol), Pd(PPh₃)₄ (23 mg, 5 mol %), and K₂CO₃ (886.7 g, 6.416 mmol) were added under an argon atmosphere. A previously degassed mixture of toluene and water (9 mL toluene: 3 mL water) was injected into the reaction mixture and purged with argon for 40 minutes. The mixture was vigorously stirred at 95 °C for 3 days. After this period, the precipitate was collected by filtration and washed thoroughly with water, followed by methanol and chloroform. Subsequently, the precipitate underwent additional washing with methanol, acetone, and chloroform in a Soxhlet apparatus. Each solvent was subjected to

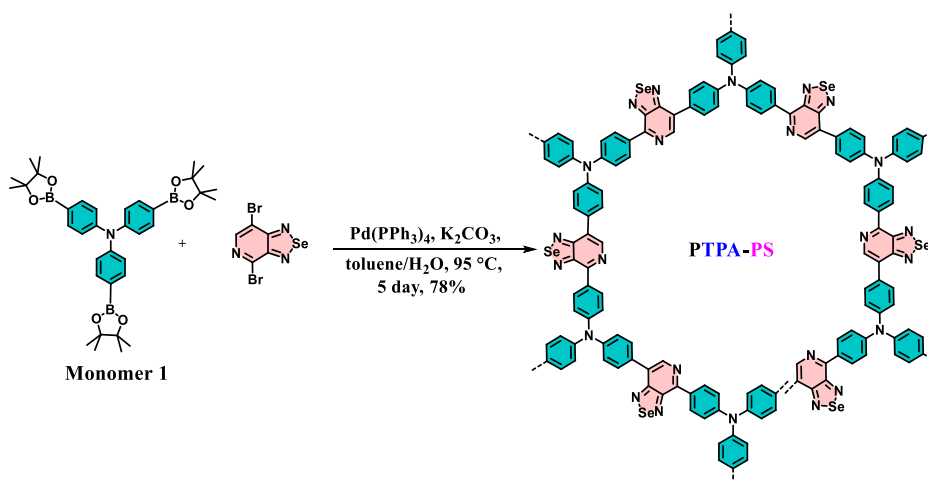
Soxhlet purification for 1 day. Finally, the polymer was dried under vacuum to yield a reddish-brown product (170 mg) with a 95% yield. FT-IR: 1593, 1509, 1476, 1318, 1279, 821, 510 cm^{-1} ; TGA: 5% weight loss at 354 $^{\circ}\text{C}$.



Scheme S1. Synthesis of PTPA-BT.



Scheme S2. Synthesis of PTPA-BS.



Scheme S3. Synthesis of PTPA-PS.

2. Characterization:

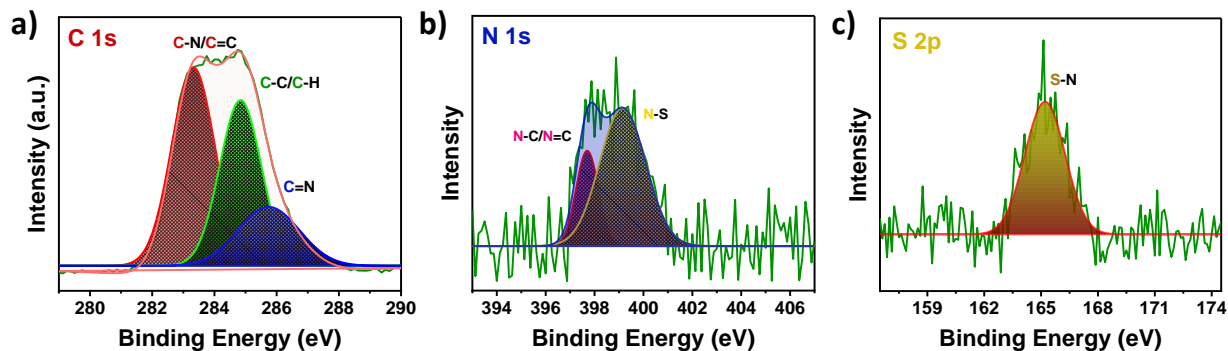


Figure S1. High-resolution deconvoluted XPS spectra of (a) C 1s, b) N 1s and c) S 2p for PTPA-BT.

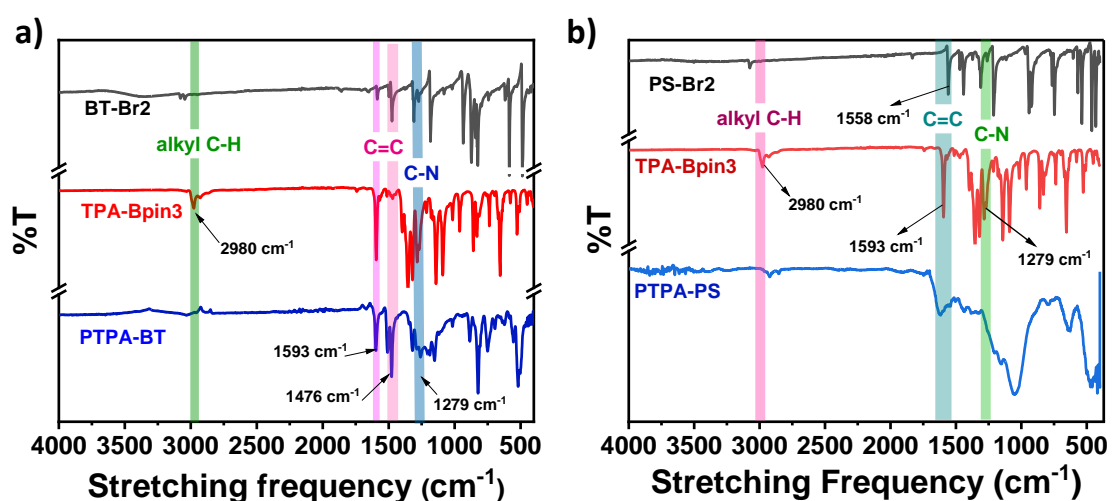


Figure S2. FT-IR spectra of a) monomer BT-Br2 (black), monomer TPA-Bpin3 (red) and polymer PTPA-BT (blue); and b) monomer PS-Br2 (black), monomer TPA-Bpin3 (red) and polymer PTPA-PS (blue).

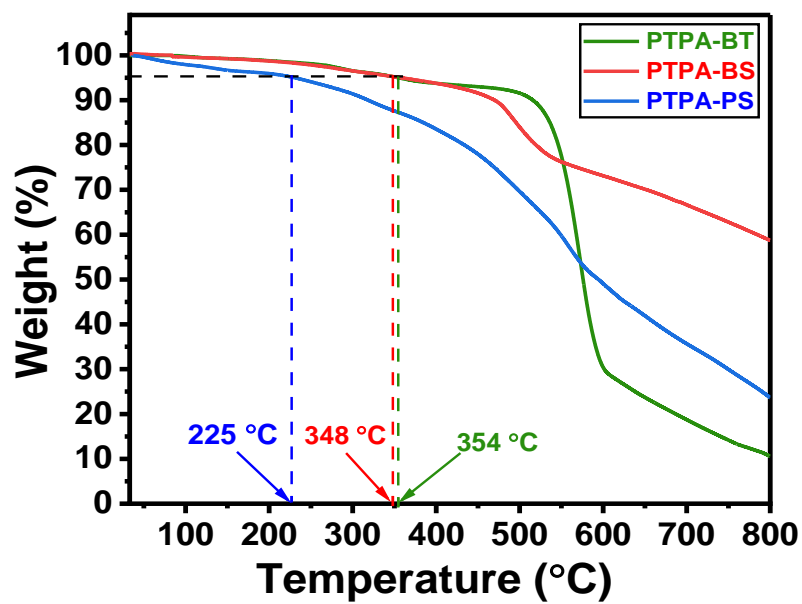


Figure S3. TGA curves for three CMPs at nitrogen atmosphere.

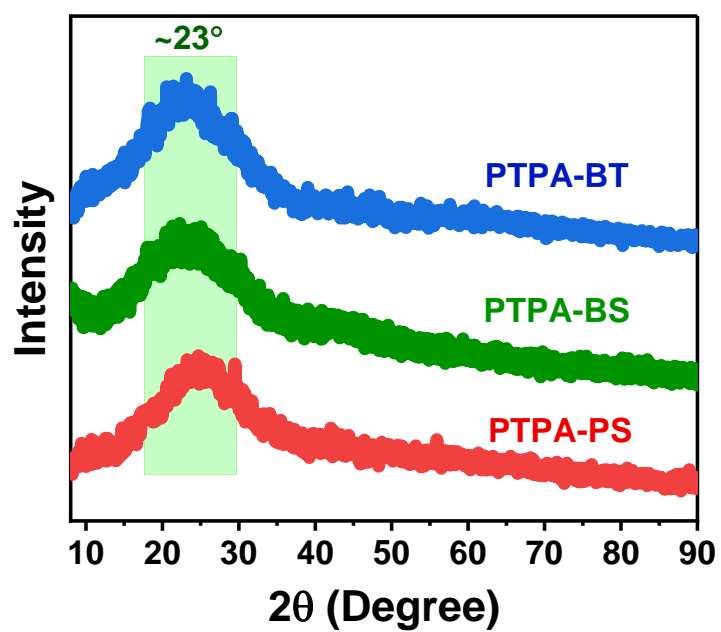


Figure S4. PXRD patterns of the CMPs.

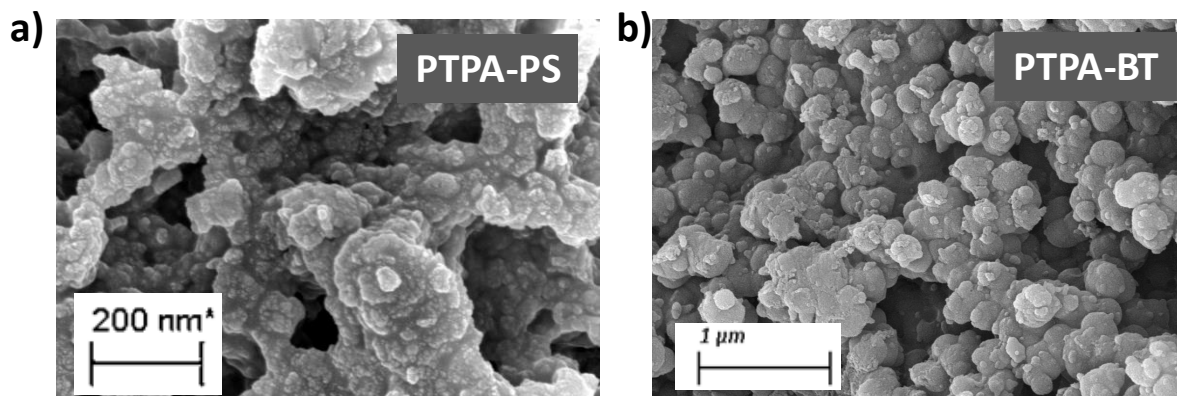


Figure S5. SEM images of **PTPA-PS** and **PTPA-BT**.

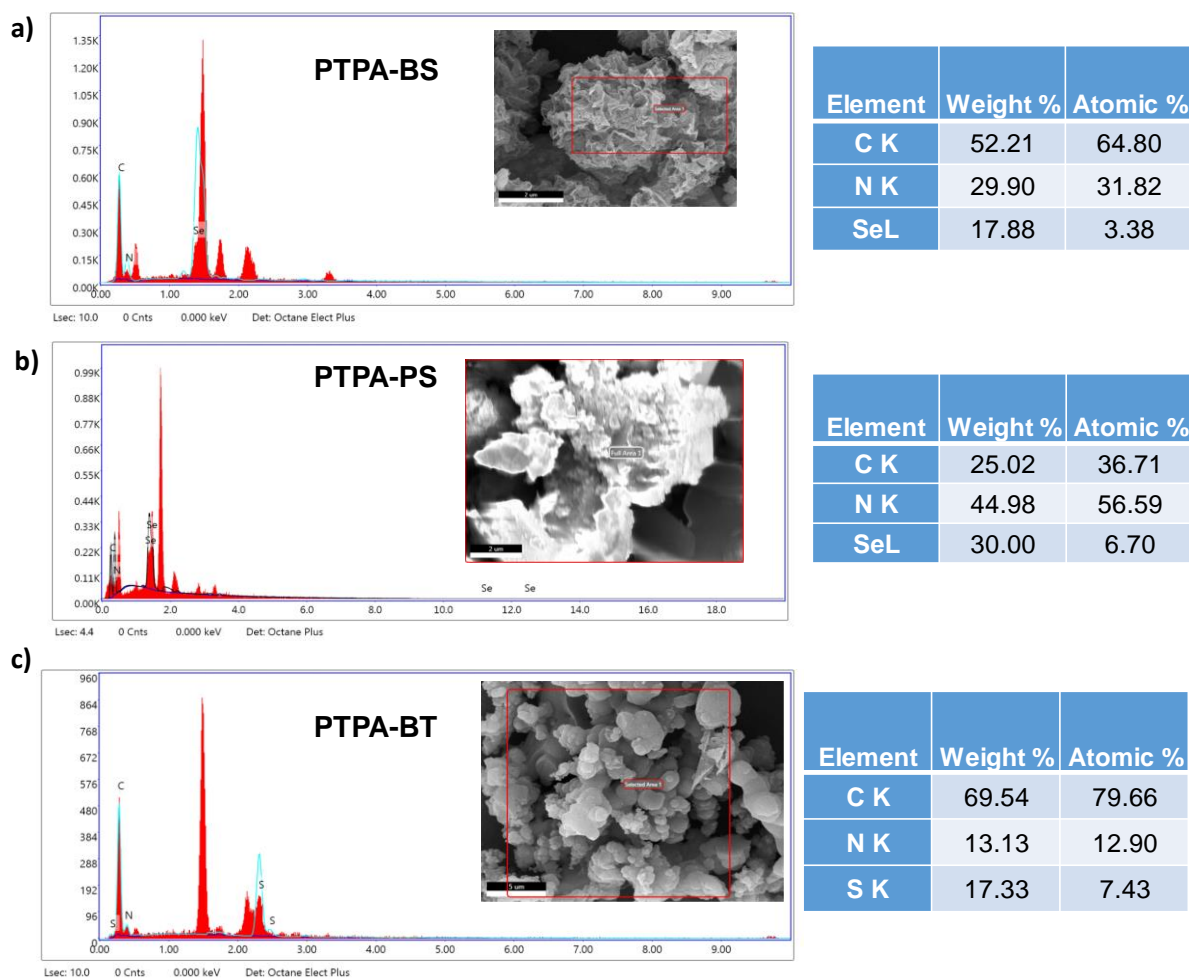


Figure S6. Energy dispersive X-ray (EDX) analysis of a) **PTPA-BS**, b) **PTPA-PS** and c) **PTPA-BT** coupled with scanning electron microscopy; inset: tabular representation of different elements in atomic% and weight% present in the polymer.

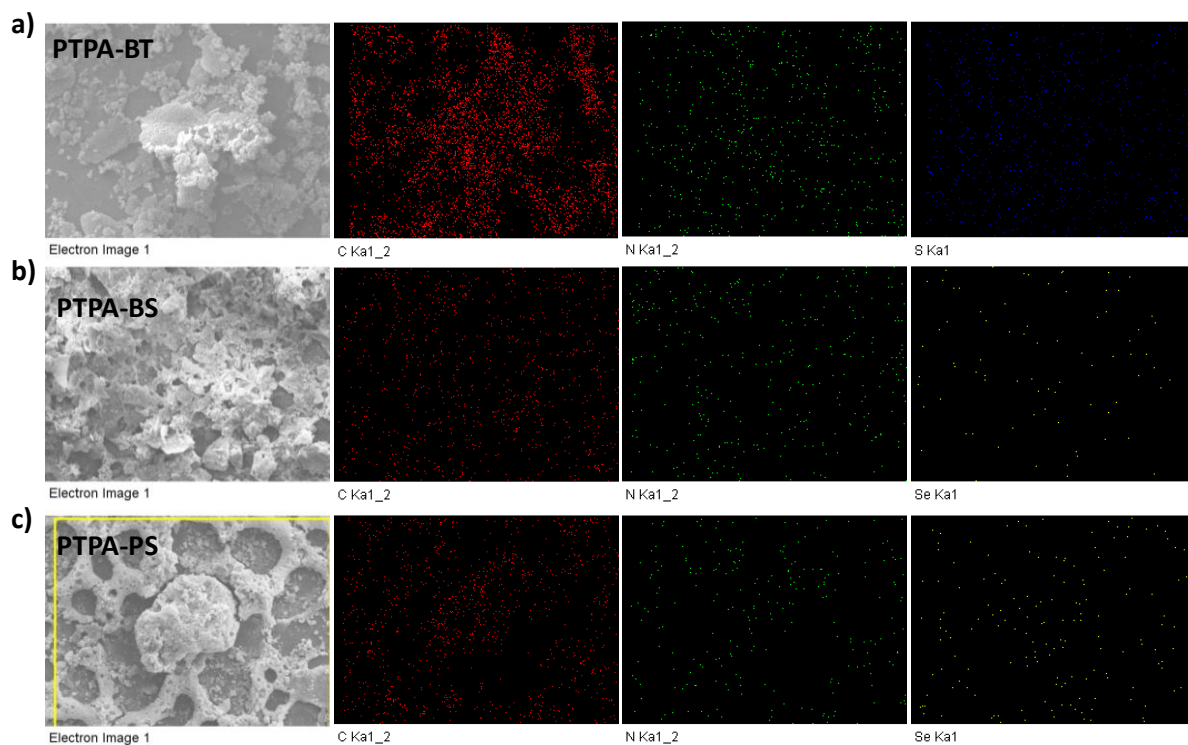


Figure S7. Elemental mapping analysis of a) PTPA-BT, b) PTPA-BS and c) PTPA-PS.

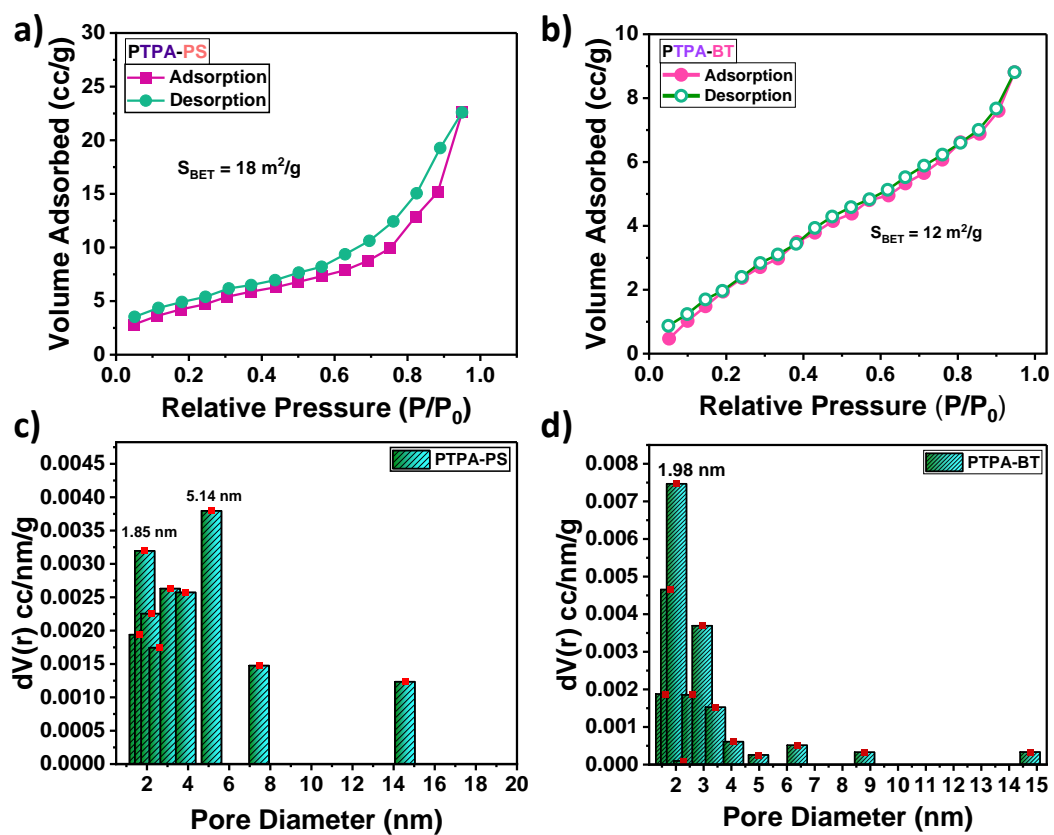


Figure S8. Nitrogen adsorption-desorption isotherms of a) PTPA-PS and b) PTPA-BT at 77 K; and their corresponding pore size distribution curves of c) PTPA-PS and d) PTPA-BT.

Table S1. BET surface area, pore volume and average pore diameter of the CMPs.

CMPs	BET Surface Area	BJH Adsorption cumulative volume of pores	BJH Adsorption average pore diameter
PTPA-BS	85 m ² /g	0.0306 cm ³ /g	3.3491 nm
PTPA-PS	18 m ² /g	0.0313 cm ³ /g	5.1422 nm
PTPA-BT	13 m ² /g	0.0114 cm ³ /g	2.0262 nm

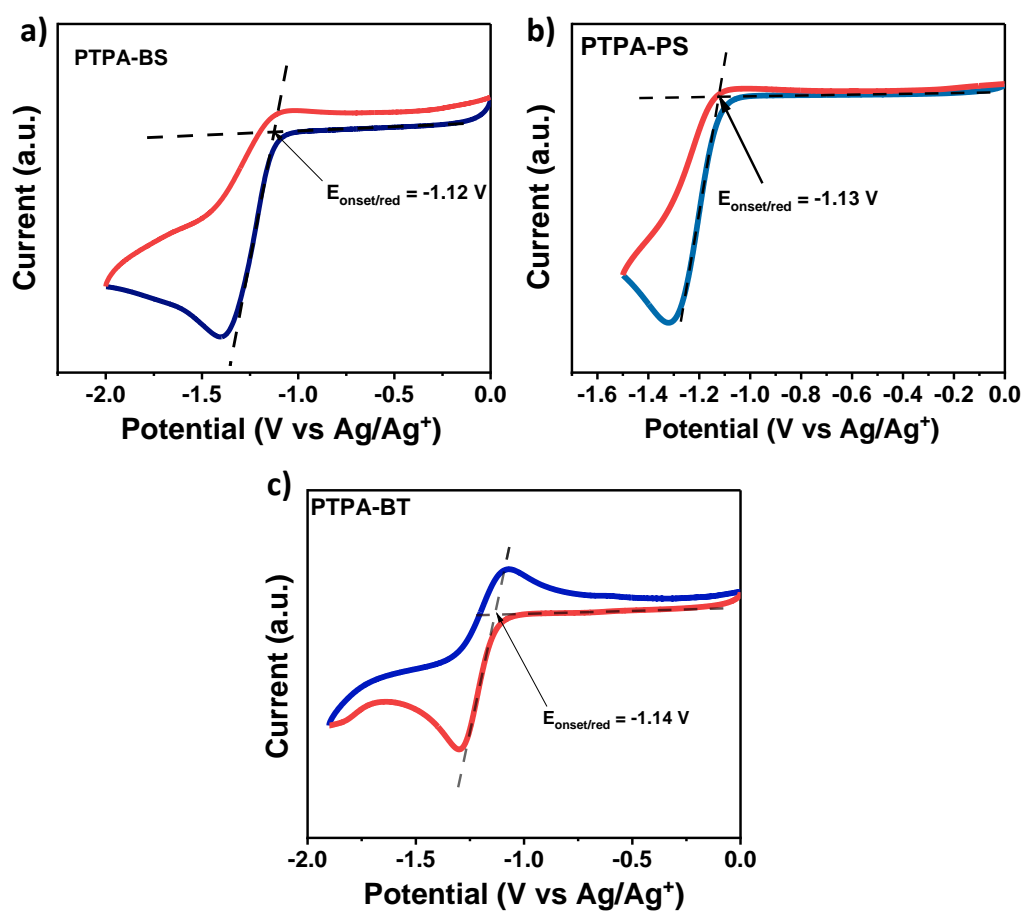


Figure S9. CV plots of PTPA-BS, PTPA-PS and PTPA-BT.

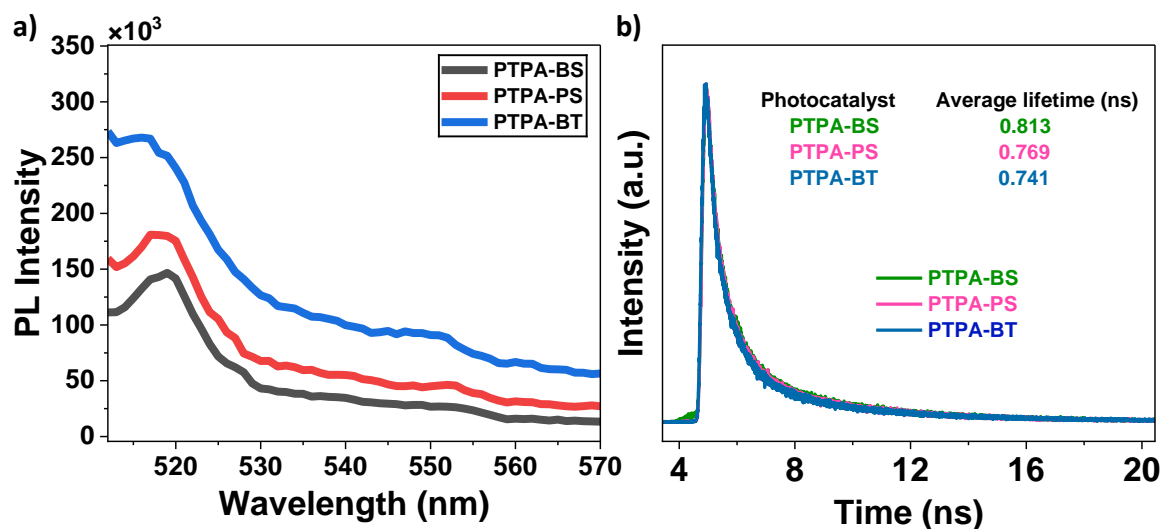


Figure S10. a) Photoluminescence spectra (PL, excited at 450 nm) and b) photoluminescence decay measurements of the as-prepared CMPs.

3. Photocatalytic Applications

3.1. Photocatalytic oxidation of aryl sulfides

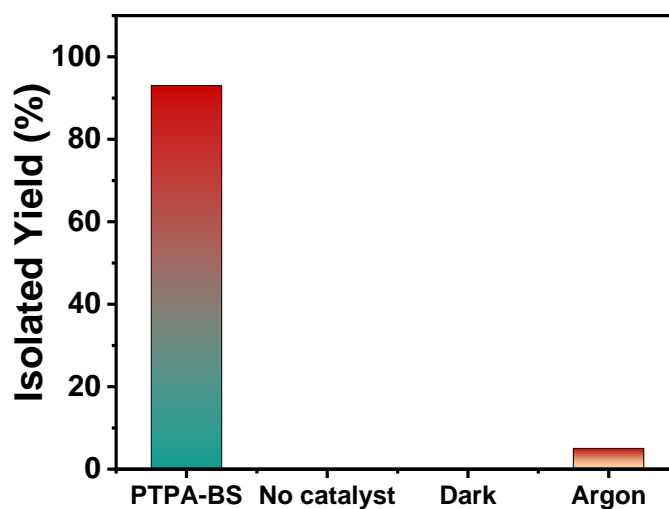


Figure S11. Control tests for oxidation of thioanisole by PTPA-BS.

Table S2: Comparison of the catalytic activity of our photocatalyst with other conventional catalysts for the oxidation of thioanisole.

Entry	Catalyst	Reagent	Temperature (°C)	Solvent	Reaction Time	Yield (%)	References
1	C ₄₂ H ₃₄ N ₈ O ₈ SnZn ₂ .C ₃ H ₇ NO.4H ₂ O.4N O ₃)	Oxygen	RT	MeOH, DCM	12 hours	100	<i>Inorganic Chemistry</i> 2011 , 50, 5318-5320 Xie <i>et al.</i> ⁵
2	Ferric bromide	Hydrogen Peroxide	RT	MeOH/H ₂ O	5 hours	100	<i>Inorganic Chemistry Communications</i> 2013 , 28, 52-54 Villalobos <i>et al.</i> ⁶
3	Gold (chitosan/silica nanocatalyst)	Hydrogen Peroxide	60	MeOH/H ₂ O	5 min	100	<i>Catalysis Communications</i> 2015 , 72, 142-146 Wang <i>et al.</i> ⁷
4	Alumina , Tris(2,2'-bipyridyl)ruthenium(II) chloride	Oxygen	RT	Acetonitrile	12 hour	100	<i>Journal of the American Chemical Society</i> 2017 , 139, 269-276. Leow <i>et al.</i> ⁸
5	12-Tungstophosphoric acid	-	95	water	10 min	100	<i>Reaction Chemistry & Engineering</i> 2023 , 8, 538-542 Mueller <i>et al.</i> ⁹
6	Cerium molybdenum oxide	Hydrogen Peroxide	20	-	8 min	100	<i>Applied Organometallic Chemistry</i> 2019 , 33, e5237 Feghhi <i>et al.</i> ¹⁰
7	Bismuth Oxybromide (BiOBr)	Hydrogen Peroxide (H ₂ O ₂)	60	Acetonitrile	7 hours	100	<i>Advanced Functional Materials</i> 2023 , 33, 2213935. Sen <i>et al.</i> ¹¹
8	PTPA-BS	Molecular Oxygen (O ₂)	RT	MeOH/H ₂ O	12 hours (100 W white LED)	93	Our work

Table S3. Photocatalytic conversion of sulfide compounds to less toxic sulfoxides using porous materials as photocatalysts.

Porous Materials	Reaction condition	Time	Conversion	Reference
CMP-BDD	Sulfide (1 mmol), HCl (4 mL, 20 mol%), O ₂ , 14 W blue LED, RT	24 h	>99%	<i>ChemPhotoChem</i> , 2019 , 3, 645–651 Zhang <i>et al.</i> ¹²
TCP-CPMP	Sulfide (0.5 mmol), CH ₃ CN/H ₂ O (10 mL, 1 : 1 v/v), O ₂ (1 atm), 100 W white LED, 25 °C	16 h	99%	<i>ChemCatChem</i> , 2020 , 12, 3523–3529 Jiang <i>et al.</i> ¹³
BN@TTCOP	Sulfides (0.2 mmol), methanol (3.0 mL), O ₂ (1 atm), white LED lamp, RT	7 h	>99%	<i>Appl. Catal., B</i> , 2020 , 277, 119274 Lan <i>et al.</i> ¹⁴
PyPor-COF (1.0 mg)	Sulfides (0.2 mmol), H ₂ O (2.0 mL), Red LEDs (5 W, 660 nm), RT	24 h	99%	<i>ACS Catal.</i> 2024 , 14, 2631–2641 Niu <i>et al.</i> ¹⁵
I-POP (10 mg)	Sulfides (0.3 mmol), MeOH (2.0 mL), Red LEDs (5 W, 660 nm), RT	10 h	97%	<i>Small</i> , 2023 , 19, 2302045 Paul <i>et al.</i> ¹⁶
4F-COF (10 mg)	Sulfides (0.2 mmol), 1.4 mL CH ₃ CN + 0.6 mL MeOH, RT = 25 ± 2 °C, O ₂ (~0.1 MPa), 14 W LED lamp (0.20 W/cm ²)	12 h	100%	<i>Small</i> 2024 , 2405550 Xie <i>et al.</i> ¹⁷
4H-COF (10 mg)	Sulfides (0.2 mmol), 1.4 mL CH ₃ CN + 0.6 mL MeOH, RT = 25 ± 2 °C, O ₂ (~0.1 MPa), 14 W LED lamp (0.20 W/cm ²)	12 h	16%	<i>Small</i> 2024 , 2405550 Xie <i>et al.</i> ¹⁷
PTPA-BS (2 mg)	Sulfides (0.2 mmol), MeOH/H ₂ O (3.0 mL), 100 W white LEDs	12 h	>99%	This work

Table S4: Comparison of photocatalytic activity for our as-synthesized CMPs under different light sources.

Illumination Wavelength	Yield (%)		
	PTPA-BS	PTPA-PS	PTPA-BT
Blue light (380-500 nm)	82	65	43
Green light (500-600 nm)	30	26	22
Red light (620-750 nm)	20	17	11

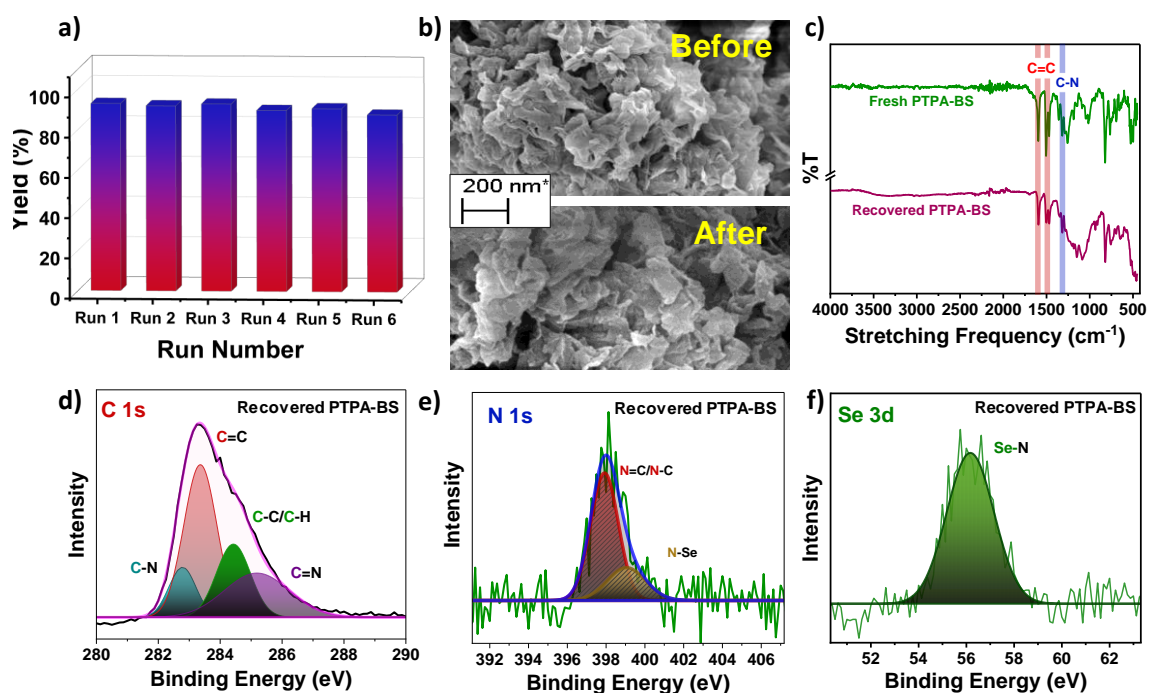


Figure S12. a) Reusability of PTPA-BS in photo-oxidation of thioanisole; b) SEM images of fresh recovered PTPA-BS; c) FT-IR spectra of recovered PTPA-BS after 6th run in comparison with fresh PTPA-BS; high-resolution deconvoluted XPS spectra of d) C 1s, e) N 1s and f) Se 3d for recovered PTPA-BS after 6th run.

References

1. K. Akatsuka, G. Takanashi, Y. Ebina, M.-a. Haga and T. Sasaki, *J. Phys. Chem. C*, 2012, **116**, 12426-12433.
2. W. Zhou, J. Jia, J. Lu, L. Yang, D. Hou, G. Li and S. Chen, *Nano Energy*, 2016, **28**, 29-43.
3. H. Xu, X. Li, H. Hao, X. Dong, W. Sheng and X. Lang, *Appl. Catal. B: Environ.*, 2021, **285**, 119796.
4. S. Sau, F. Banerjee and S. K. Samanta, *ACS Appl. Nano Mater.*, 2023, **6**, 11679-11688.
5. M.-H. Xie, X.-L. Yang, C. Zou and C.-D. Wu, *Inorganic Chemistry*, 2011, **50**, 5318-5320.
6. L. Villalobos and T. Ren, *Inorganic Chemistry Communications*, 2013, **28**, 52-54.
7. F. Wang, C. Liu, G. Liu, W. Li and J. Liu, *Catalysis Communications*, 2015, **72**, 142-146.
8. W. R. Leow, W. K. H. Ng, T. Peng, X. Liu, B. Li, W. Shi, Y. Lum, X. Wang, X. Lang, S. Li, N. Mathews, J. W. Ager, T. C. Sum, H. Hirao and X. Chen, *Journal of the American Chemical Society*, 2017, **139**, 269-276.
9. P. Mueller, A. Vriza, A. D. Clayton, O. S. May, N. Govan, S. Notman, S. V. Ley, T. W. Chamberlain and R. A. Bourne, *Reaction Chemistry & Engineering*, 2023, **8**, 538-542.
10. A. Feghhi, R. Malakooti and S. Malakooti, *Applied Organometallic Chemistry*, 2019, **33**, e5237.
11. Z. Shen, Z. Luo, J. Chen and Y. Li, *Advanced Functional Materials*, 2023, **33**, 2213935.
12. H. Zhang, Q. Huang, W. Zhang, C. Pan, J. Wang, C. Ai, J. Tang and G. Yu, *ChemPhotoChem*, 2019, **3**, 645-651.
13. J. Jiang, Z. Liang, X. Xiong, X. Zhou and H. Ji, *ChemCatChem*, 2020, **12**, 3523-3529.
14. X. Lan, Q. Li, Y. Zhang, Q. Li, L. Ricardez-Sandoval and G. Bai, *Appl. Catal. B: Environ.*, 2020, **277**, 119274.
15. K.-K. Niu, T.-X. Luan, J. Cui, H. Liu, L.-B. Xing and P.-Z. Li, *ACS Catal.*, 2024, **14**, 2631-2641.
16. R. Paul, P. Kalita, D. Q. Dao, I. Mondal, B. Boro and J. Mondal, *Small*, 2023, **19**, 2302045.
17. Q. Xie, A. Chen, Z. Gao, S. Gu, B. Wei, R. Liang, F. Zhang, Y. Zhao, J. Tang, C. Pan and G. Yu, *Small*, 2024, **n/a**, 2405550.